Int. J. Electrochem. Sci., 16 **(2021)** 150969, doi: 10.20964/2021.01.15

International Journal of
ELECTROCHEMICAL
SCIENCE
www.electrochemsci.org

Investigation of Anodic Behavior of Nickel in H_2SO_4 Solutions Using Galvanostatic Polarization Technique. I. Kinetics and Thermodynamic Approach

S. Abd El Wanees[1,2,], M.Abdallah[3,4], Arej S Al-Gorair[5], F.A.A. Tirkistani[3], S. Nooh[6], R. Assi[7]*

[1] University College of Umluj, Umluj, Tabuk University, Tabuk, Saudi Arabia.
[2] Chemistry Department, Faculty of Science, Zagazig University, Zagazig, Egypt
[3] Chemistry Department, Faculty of Science, Umm Al-Qura University, Makkah Al Mukaramha, Saudi Arabia
[4] Chemistry Department, Faculty of Science, Banha University, Banha, Egypt
[5] Chemistry Department, College of Science, Princess Nourah bint Abdulrahman University, Riyadh, Saudi Arabia
[6] University College of Umluj, Computer Science Department, Umluj, Tabuk University, Tabuk, Saudi Arabia
[7] Company of Water and Wastewater, Canal Provinces, Ismailia City, Egypt
[*]E-mail: s_wanees@yahoo.com & s_nasr@ut.edu.sa

Received: 28 September 2020 / *Accepted:* 3 November 2020 / *Published:* 30 November 2020

The electrochemical passivation behavior of Ni in H_2SO_4 solutions was studied by the galvanostatic anodic polarization method. The data of the polarization curves relied on the polarizing current, $I_{imposed}$, acid concentration, C, and the temperature, T. The polarized curve elucidated various characteristic regions confirming various oxidation processes. The 1st region is recognized by a rapid jump in the Ni electrode potential E (zone I), due to the decay of H_2 over-voltage. A large discrete 1st potential arrest, ***a***, coincides with the formation of Ni^+ ions, while the 2nd potential arrest, ***b***, matches the electro-oxidation of Ni^+ ions to Ni^{2+} ions. The second increase in the potential, E (zone II), harmonizes the onset of passivity due to the countenance of Ni_2O_3. The duration time, τ, of the two arrests ***a*** and ***b*** decrease with increasing the $I_{imposed}$, T, and the acid concentration, C. The thermodynamics activation parameters, E_a, ΔH_a, and ΔS_a for the dissolution and passivation processes are deduced and discussed.

Keywords: Nickel; Anodic polarization; Dissolution; Thermodynamic; Oxide film; Passivity; Kinetics.

1. INTRODUCTION

Ni and Ni-alloys manifest good reluctance towards the corrosion in different aqueous solutions owing to the existence of a stable passive oxide layer on the outer surface of the Ni metal [1-7]. The ease

of formation of the passive film depends on numerous parameters among which is the concentration, presence of aggressive anion, temperature and *p*H of the solution [8-11], as well as, on the metal structure [12, 13]. Nickel is utilized in various energy-industrializing cells, in which aqueous or non-aqueous electrolytes are employed. The good corrosion resistance of nickel in aqueous media could be specified in its compact oxide film [14]. The study of this oxide film has taken specified importance from several investigators. The nickel oxide nature was reported to be potential-dependent [15-17] with composition varied with the immersion time [18].

A few attentiveness has been focused on the study of the potentiostatic of Ni electrode in solutions initially free from Ni [19, 20]. An intermediate layer composed of $NiOH_{ads}$ is formed on the Ni surface by a solid-state mechanism. Beneficial knowledge about the kinetics of the film development on the metal could be acquired from the way of the open-circuit potential changes with the inundation time. However, little information is available about the extent of tolerance of corrosive anions before the breakdown of the passive layer on the nickel surface and the probable initiation of general or localized corrosion. In acidic media, the Ni metal could be oxidized to dissolve as divalent cations with the production of hydrogen gas. Practically, the tolerance to the corrosion of nickel in acidic media is higher than that specified by the *E*-*p*H equilibrium diagrams [21].

Otherwise, the presence of nickel in the electrochemical series, which is considered as mild active concerning the H^+/H equilibrium. Furthermore, the passivity of nickel is assigned to the presence of a protective oxide layer or a hydrated oxide layer [22] or a chemisorbed film of oxygen [23]. Bockris et al. [24] have assigned that the resistance of nickel towards the corrosion in acid solution is attributed to the rise in the conductivity of the formed oxide. The potentio-kinetic polarization curves of Ni by some researchers indicated considerable conflicts [25-27]. Such incongruities were related to the nature and the number of imperfections of each of the metal and the electrolyte under test [25, 26].

The electrochemical attitude of Ni in acidic media was found to depend on various factors among these is the acid concentration [27-29]. The passivity of Ni in sulfuric acid solutions was assumed to be in two phases [24, 30]. The first layer formed is electrically non-conducting which posteriorly transformed into an electronically conducting passivated layer of NiO. The current investigation aims to highlight the kinetics of the dissolution and passivation processes of Ni surface in various concentrations of H_2SO_4 solutions, by galvanostatic polarization technique. The influence of the imposed current density, $I_{imposed}$, and the temperature on the polarization curves are examined and some thermodynamic activation functions are deduced and discussed.

2. MATERIALS AND METHODS

2.1. Materials

The pure Ni electrode (*WE*) used in our study was severed from a homogenous cylindrical rod (Johnson and Matthey-England). A thick Cu-wire was interfused with the end of the prepared Ni rod for electrical connection. The rod was reinforced into a Pyrex glass tube using a suitable resin (Araldite) leaving an exposed free surface of a cross-section area of 0.97 cm^2 to be in touch with the examined

electrolyte. Before carrying the experiment, the surface area of the *WE* was mechanically abraded using various grades of soft emery papers to remove any pre-immersion oxide films or roughness, degreased with acetone, followed by washing with distilled water. The surface pretreatment was done before each run and directly immersed in the freshly prepared solution.

2.2. The Electrolytic cell

The three-electrode electrolytic cell, which consists of two compartments connected through a fitted glass disc to prohibit the mixing of the two solutions together [31-34]. The cell has a double jacket through which water was circulated. The different electrodes were a Pt wire as a subsidiary electrode, Ni as a *WE*, and a saturated calomel electrode (SCE) as a reference electrode with a Luggin capillary focused on the *WE* surface.

The acid solutions were prepared from A.R. H_2SO_4 and a bi distilled water. Experiments were done at room temperature, 25±1ºC, except those carried out at different temperatures. The cell temperature was adjusted by utilizing an ultra-thermostat-type Poly Science (USA). Every run was done with a newly polished electrode sample and a freshly prepared solution. Polarization data were collected on a recorder unit, Cole Parmer Instruments (USA).

3. RESULTS AND DISCUSSION

3.1. The influence of current

Figs 1 and 2 show the galvanostatic anodic polarization curves of Ni in 0.01M and 0.10 M H_2SO_4 solutions, respectively, at 25ºC.

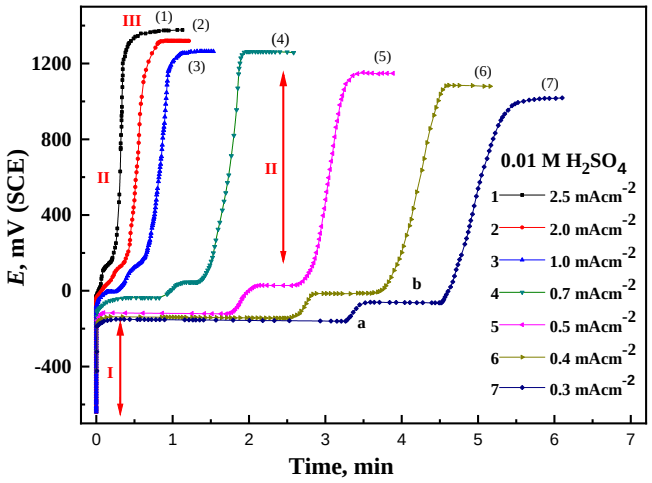

Figure 1. Galvanostatic anodic polarization curves of Ni in 0.01 M H_2SO_4 solution, at different current densities, (2.5 - 0.3 $mAcm^{-2}$), at 25ºC.

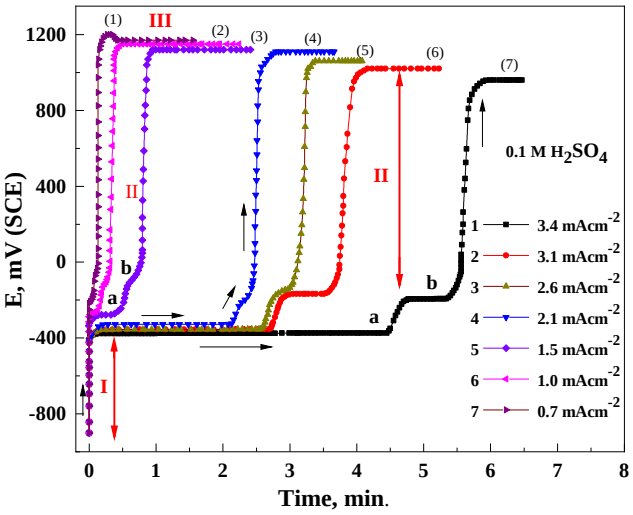

Figure 2. Galvanostatic anodic polarization curves of Ni in 0.1 M H_2SO_4 solution, at different current densities, (3.4 - 0.7 $mAcm^{-2}$), at 25°C.

The polarization curves were carried out under different applied current densities, $I_{imposed}$. The data of the curves are characterized by a rapid and roughly linear change of the electrode potential *E* (zone I) due to the decay of the H_2 overvoltage on the Ni electrode surface and followed by charging of the electrical double layer at the Ni/solution interface [35-39]. Such a step occurs through a potential range varied between -0.9 and -0.25 V_{SCE} depending on the extent of the used $I_{imposed}$ and the solution concentration [36, 37]. Posterior to the decay step (zone I), the *E* of the Ni electrode varies tardily with reaction time to afford a relatively large distinct arrest, ***a***, pursued by a small one, ***b***. The duration of arrests ***a*** and ***b*** are increased as the applied current density is lowered.

However, by congruence with the previous studies, when the *E* of the Ni electrode is sweeping within the region of the arrest, ***a***, Ni is ready to oxidize through losing one electron to give Ni^+ ions followed by the electro formation of divalent cation species, Ni^{2+} ions, which is characterized by the arrest, ***b***. According to the literature [40-42] the reactions occurring during arrests ***a*** and ***b*** can be represented by equations 1and 2, successively:

$$Ni \rightarrow Ni^+ + e \quad (1)$$

an/or

$$Ni^+ \rightarrow Ni^{2+} + e \quad (2)$$

$$Ni^{2+} + H_2O \rightarrow NiO + 2H^+ + e \quad (3)$$

Since NiO is a non-ionic oxide, slightly soluble, the potential along the second arrest ***b*** stays more/or less constant for an assured period, which depends on the applied current densities and the solution composition. It is presumed that the electro-oxidation of Ni^+ ions to the divalent form, Ni^{2+} ions, (reaction 2) continues at a rate equal to the rate of oxide film formation (oxidation of Ni^{2+} to NiO, reaction 3). This step is continued until the active oxidation of Ni is mainly restrained. The jump in the potential into the positive direction after the second arrest ***b*** could be attributed to the precipitation of nickel oxides on the Ni surface, producing the passive film. At this process, a sufficient oxide has

compiled and its rate becomes higher than that of metal dissolution [43]. However, many authors coincided that the passive layer is composed of two oxide-layers in the *E* region of Ni^{2+} ions. This film is consists of an inner NiO layer and an outer $Ni(OH)_2$ layer[44]. The data explored by Melendres and Pankuch [45], based on surface-enhanced Raman spectroscopy studies display the existence of both $Ni(OH)_2$ and NiO involved in the passive film formed on the Ni surface in presence of different *p*H solutions. Oblonsky and Devine utilizing surface-enhanced Raman spectroscopy [46] and reported the presence of amorphous $Ni(OH)_2$ layer on the nickel electrode when immersed in a borate buffer solution. Nishimura et al. [42] also proved the bi-layer constructer of the nickel passive layer. At low *p*H values, some authors confirm the presence of more than two oxides on the passive film, such as NiO, Ni_2O_3, and Ni_3O_4 [47-49].

However, the constancy in the potential during the region of the arrest relied on the H_2SO_4 concentration, *C*, as well as the applied current, $I_{imposed}$, Figs 1 and 2. This signifies that at the low current density during the anodic arrest ***a***, the rate of dissolution of Ni is very low and the corrosion products are freely soluble in the solution at a rate equal to or even faster than the rate of oxide formation [38]. Upon further increase of the $I_{imposed}$, the anodic potential rises, zone II. During these relatively higher current densities, the rate of oxide film formation during region II is much faster than that of Ni dissolution. Finally, the electrode potential reaches the passive value, which corresponds to the oxygen evolution potential, zone III.

Table 1. The values of the constants α (mV), α' (mV), α" (mV), β (mV/decade), β' (mV/decade) and (β"/decade) of equations 4 and 5.

Solution	α, mV	α', mV	α", mV	β, mV/decade	β', mV/decade	β", mV/decade
0.01 M H_2SO_4	-66	89	1200	185	210	342
0.10 M H_2SO_4	-303	-155	1000	185	210	342

Figs 3 and 4 show the variation in the dissolution potential of the Ni electrode at arrest ***a***, E_1, in mV and arrest ***b***, E_2, in mV and the applied current, log $I_{imposed}$, in mA/cm^2, respectively. It is obvious that, as the polarizing current density, $I_{imposed}$, increases the potential corresponding to the arrests ***a*** and ***b*** (E_1 and E_2) shifts to the less active direction, more positive values, following the equation:

$$E_{1(2)} = \alpha\,(\alpha') + \beta(\beta')\log I_{imposed} \qquad (4)$$

where α (α') and β (β') are constants that depend on the electrolyte concentration. The constants β and β' which are the slopes of lines relation of Figs 3 and 4 are equal to 180 and 240 mV decade^{-1}, successively. This confirms that the oxidation processes during the two arrests ***a*** and ***b*** take place through the same mechanism in different concentrations of H_2SO_4. The values of the constants α and α' of equation 4 are considered to depend on H_2SO_4 amounts and represent the dissolution potentials, E_1, E_2, at 1.0 mA/cm^2, and take the values -66, (-303) and 89, (-155) mV decade^{-1}, successively, Table 1.

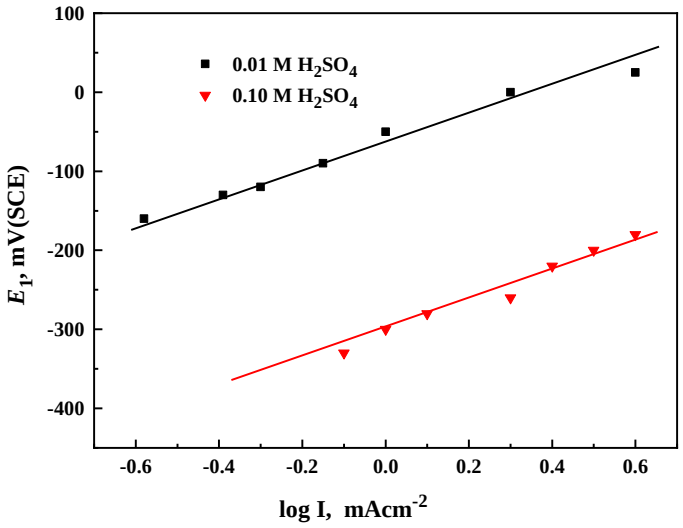

Figure 3. Variations of the oxidation potential, E_1, with the applied current density, log $I_{imposed}$, at 25°C.

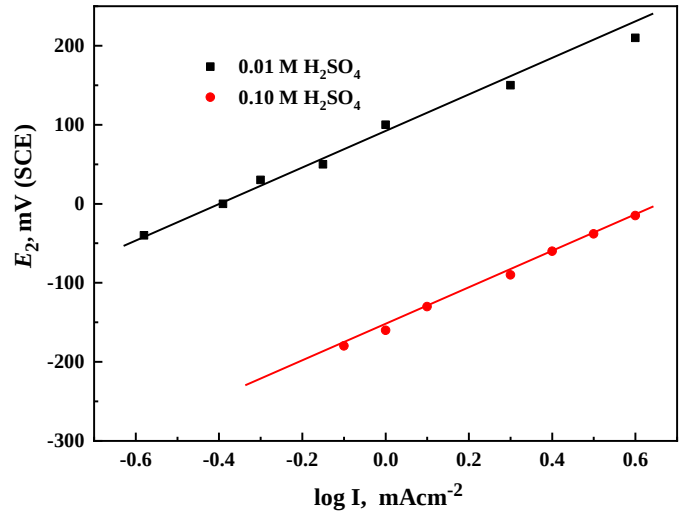

Figure 4. Variation of the oxidation potential, E_2, with the applied current density, log $I_{imposed}$, at 25°C.

Finally, at the end of zone II of the polarization curves of Figs 1 and 2, the potential is swerved from linearity, zone III, to attain the steady-state of the oxygen evolution (E_{oxygen}) that relies on the H_2SO_4 amounts, C, and $I_{imposed}$. Fig 5 shows the relation between E_{oxygen}, in mV, and the log $I_{imposed}$, in mA/cm^2, in 0.01 M and 0.10 M H_2SO_4. It is conspicuous that the rise in the polarizing current density, $I_{imposed}$, displaces the E_{oxygen} into the noble direction, following the equation:

$$E_{oxygen} = \alpha'' + \beta'' \log I_{imposed} \quad (5)$$

where α" and β" are constants, Table 1. The value of the slope β" of the nearly parallel lines of Fig 5 is ~ 331 mV/decade. This confirms that the oxygen evolution step during this region for the different

concentrations of H_2SO_4 is completed through a similar mechanism. The constant α" of Eq 5 is noticed to be concentration-dependent (Table 1) and has a value of 1200 and 1000 mV/decade, for $1x10^{-2}$ M and $1x10^{-1}$ M H_2SO_4, successively. It is noteworthy to see that the duration of the arrests ***a*** and ***b*** in region **II** was formerly noticed, under similar experimental situations and known as the passivation or incubation period for the passivation process [36-39].

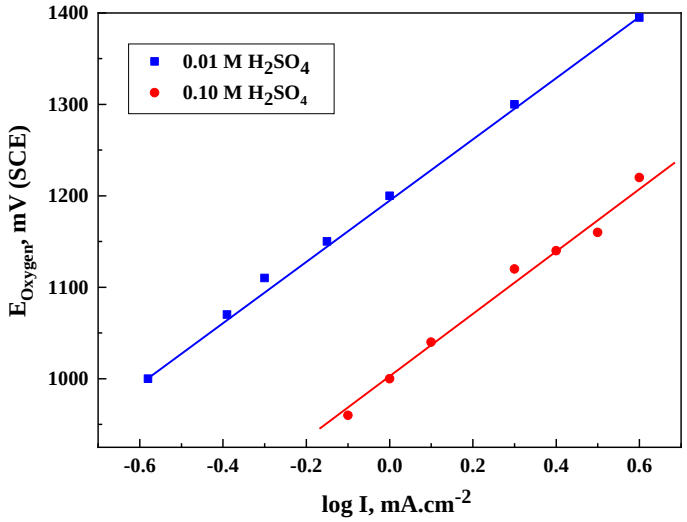

Figure 5. Variation of the E_{oxygen}, of Ni in 0.01 M and 0.10 M H_2SO_4 solutions, with the logarithm of the imposed current density, log $I_{imposed}$.

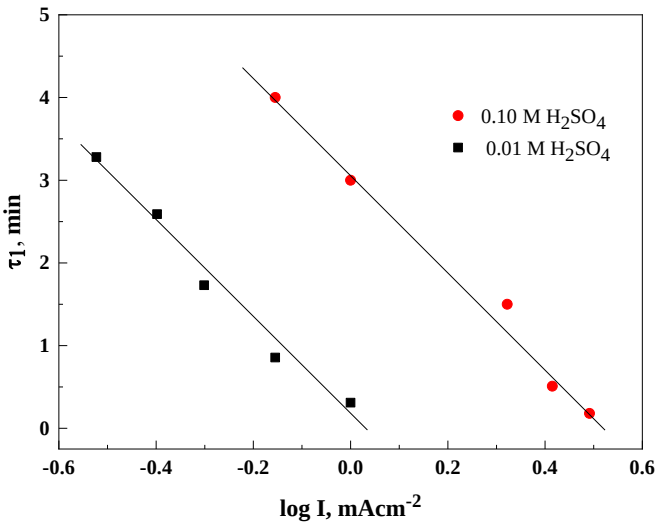

Figure 6. Variation of the duration of the potential of arrest **a,** τ_1, of Ni with the log $I_{imposed}$, in 0.01 M and 0.10 M H_2SO_4.

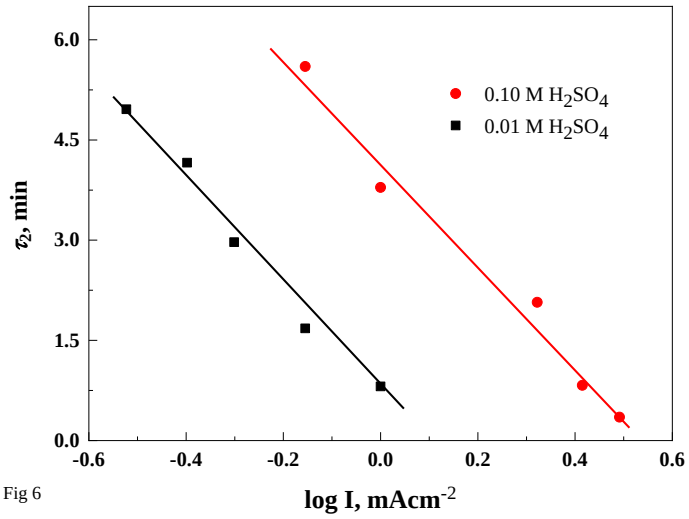

Fig 6

Figure 7. Variation of the passivation time, τ_2, of Ni with the log $I_{imposed}$, in 0.01 M and 0.10 M H_2SO_4, at 25 °C.

Table 2. The values of the constants φ_1, φ_2, m_1 and m_2 of equation 6.

Solution	φ_1, min	m_1, min/mAcm^{-2}	φ_2, min	m_2, min/mAcm^{-2}
0.01 M H_2SO_4	0.39	-5.5	0.63	-8.3
0.10 M H_2SO_4	3.09	-5.5	4.18	-8.3

The interval of the dissolution potential of arrest ***a***, τ_1 sec, and passivation process, τ_2, (duration time of the arrests ***a*** and ***b*** until O_2 evolution) relied on the $I_{imposed}$ and electrolyte concentration, *C*. As can be shown from Figs 6 and 7, the interval of the dissolution potential of the arrest ***a***, τ_1, and the passivation period, τ_2, are reduced with raising the polarizing current, $I_{imposed}$. Figs 6 and 7 confirm the relation between each of τ_1 and τ_2 with a log of $I_{imposed}$ for the nickel electrode in H_2SO_4, respectively. The data could be elucidated by the equation [36-39].

$$\log \tau_1 (\tau_2) = \varphi_{1(2)} - m_{1(2)} \log I_{imposed} \quad (6)$$

where $\varphi_{1(2)}$ and $m_{1(2)}$ are constants which is concentration-dependent. The slopes, $m_{1(2)}$, of the almost analogous straight lines of Figs 6 and 7 are found to be -5.8 and -5.8 min/mAcm^{-2} unit, for 1x10^{-2} M and 1x10^{-1} M H_2SO_4, successively.

Table 2. The values of the constants $\varphi_{1(2)}$ of equation 6 is noticed to depend on the used amount of H_2SO_4, Table 2. This might be attributed to the variance in the specific conductivity of the two different concentrations of H_2SO_4, the disproportion in the geometry of the formed passive layer, and the variance in the diffusion coefficients of the ions collaborating in the film consistency [36, 38].

Whatever, the positive shift in the potential with the reaction time, region **II** Figs 1 and 2, which is considered as a linear relation was formerly recognized with the metals forming oxides. The thickness of the formed oxide is found to be proportional to the formation potential [36, 37, 50-54]. The obtained data indicate that the thickness of the formed oxide raises with the rise in the polarizing current, $I_{imposed}$, comparable with the data obtained before [35, 42, 45, 46]. The rate of the change in the potential $(\partial E/\partial t)_i$ at a constant $I_{imposed}$ can be defined as the oxide formation rate, zone II of Figs 1 and 2. The value of $(\partial E/\partial t)_i$ is dependent on the $I_{imposed}$ by the relation [36, 37, 55, 56]:

$$(\frac{dE}{dt})_i = \lambda I_{imposed}^{n} \quad (7)$$

or

$$\log (\frac{dE}{dt})_i = \log \lambda + n \log I_{imposed} \quad (8)$$

where the symbols λ and n are considered as constants that are dependent on the type of metal under investigation[54]. Equation 8 can be graphically represented by plotting of log $(\partial E/\partial t)_i$ versus log $I_{imposed}$ for Ni immersed in 0.01 M and 0.10 M H_2SO_4 solutions. The data produces straight-line relation that are best represented by Fig 8. The value of the log λ according to equation 8 which is considered as concentrationdependent is determined to be 1.73 and 1.64 mV/s for 0.01 M and 0.10 M H_2SO_4, respectively, Table 4. On the other hand, the value of *n*, of the parallel lines, was found to be 0.83, Table 3. The work of Abd El Aal [55] found the value of *n* to be 1.2 during the study the passivation of Ni in borate solution under the galvanostatic polarization technique, while the data obtained by Ammar et al. [52], found *n* to be 1.0 if the total current is expended in the oxide film building only. The deduced value of n, which somewhat lower than unity explains that the efficacy of the ionic process is somewhat depressed than 100 %. Subsequently, a part of ionic current density is expended in the dissolution step [55]. The analogous lines of Fig 8 signalized that the oxide formation during the anodic passivation of the Ni electrode is carried by a similar mechanism in the two investigated electrolytes.

Table 3. The values of the constants λ (mV.min^{-1}) and *n* (mV.min^{-1}/ mA.cm^{-2}) of equation 8.

Concentration	log λ, mV.min^{-1}	*N*, mV.min^{-1}/ mA.cm^{-2}
0.01 M H_2SO_4	1.72	0.83
0.10 M H_2SO_4	1.64	0.83

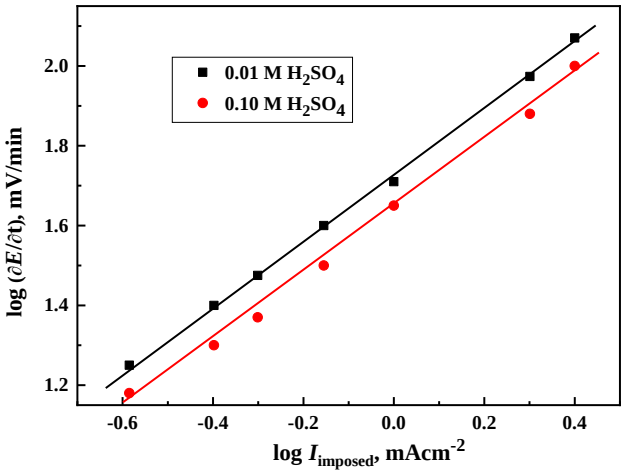

Figure 8. Variation of log ($\partial E/\partial t$) vs. log $I_{imposed}$ for Ni immersed in 1x10^{-2} M and1x10^{-1}M H_2SO_4 with log $I_{imposed}$, at 25 °C.

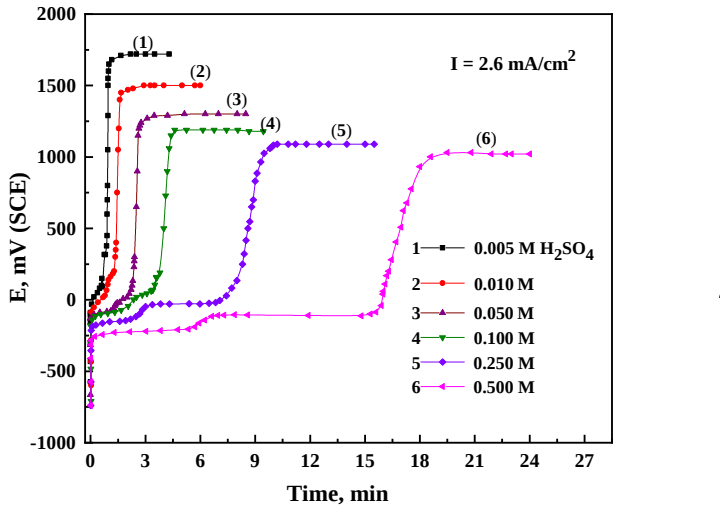

Figure 9. The anodic polarization curves of Ni in different concentrations of H_2SO_4 solutions, at 2.6 mA cm^{-2}, at 25°C.

3.2. The influence of H_2SO_4 concentration

The galvanostatic anodic polarization curves of nickel were done also in different concentrations of H_2SO_4 solutions (5x10^{-3} M to 5x10^{-1} M), when the $I_{imposed}$ equal to 2.6 mA/cm^2, at 25°C. The data obtained in Fig 9 clarify that the values of the oxidation potential corresponding to the arrests **a** and **b** (E_1, and E_2) and the interval of the passivation process, τ, was affected with the acid concentration, C. The variation of the dissolution potential corresponding to E_1 and E_2 with the electrolyte concentration, log C_{H2SO4}, is depicted in Fig 10. It is clear that the values of E_1 and E_2 are displaced to a more active direction as the amount of H_2SO_4 is raised, following the equation [35, 39].

$$E_{diss} = E^{\circ} - \frac{0.059}{Z} \log C_{H2SO4} \quad (9)$$

The obtained slopes, of Fig. 10, are amounted to be 59 and 35 mV/decade in the case of E_1 and E_2, successively. In the case of the first arrest **a**, the value of the slope 59 mV/decade refers to z = 1 (the number of e^- involved during the first dissolution step, reaction 1). With the second arrest, E_2, the value of the slope is equal to 36 mV/decade, which confirms that the number of e^- produced in the second dissolution step, arrest **b**, is two electrons (z = 2).

It is noteworthy to realize that, as the amount of H_2SO_4 solutions is raised from $5x10^{-3}$ M to $5x10^{-1}$ M the time required to form a complete passive film with O_2 evolution increases from 66 sec to 930 sec. The corresponding amount of electricity, Q_a, consumed in the passive film formation during the polarization process increases from 0.17 coulomb.cm^{-2} to 2.4 coulomb.cm^{-2}. This means that, at a constant polarizing current density, more amount of electricity, Q_a, is consumed during passive film formation on Ni at higher concentrations of H_2SO_4 due to the increase in the duration period during the dissolution step. The relation between the consumed Q_a and the concentration of H_2SO_4 solution, C, can be depicted in Fig 11. The two variables depicted a linear relationship satisfying the equation:

$$\log Q_a = a_1 - b_1 \log C \quad (10)$$

where a_1 and b_1 are constants that are dependent on the metal-type and the nature of the investigated electrolyte.

The rate of oxide film formation, $(dE/dt)_i$, was found to decrease with the rise in the acid concentrations, C, at the same the polarizing current, $I_{imposed}$, as depicted by Fig 12. Such behavior could be attributed to the increase in passive film formation as the amount of water is increased by the dilution factor.

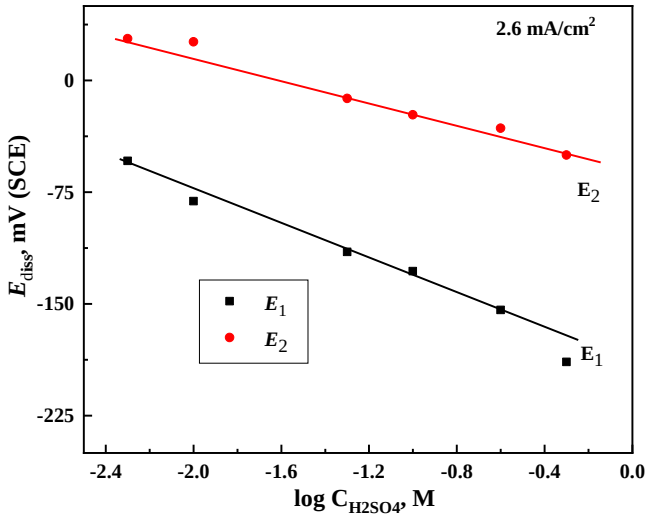

Figure 10. Variation of the dissolution potentials, E_1 and E_2, of Ni with the log C of H_2SO_4, at 25^{o}C.

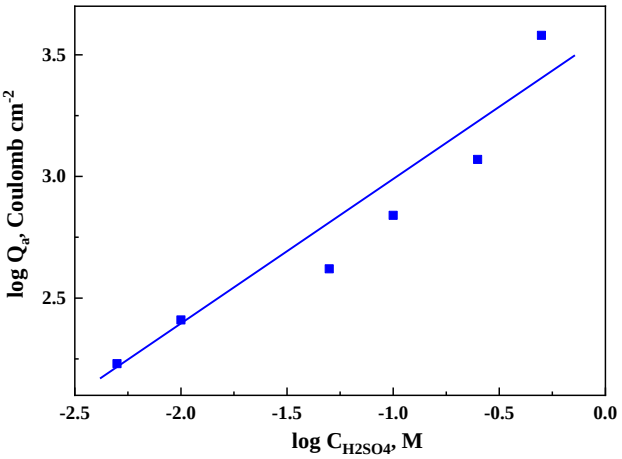

Figure 11. Variation of the quantity of electricity, Q_a, consumed for Ni passivity with the concentration of H_2SO_4 on a double logarithmic scale.

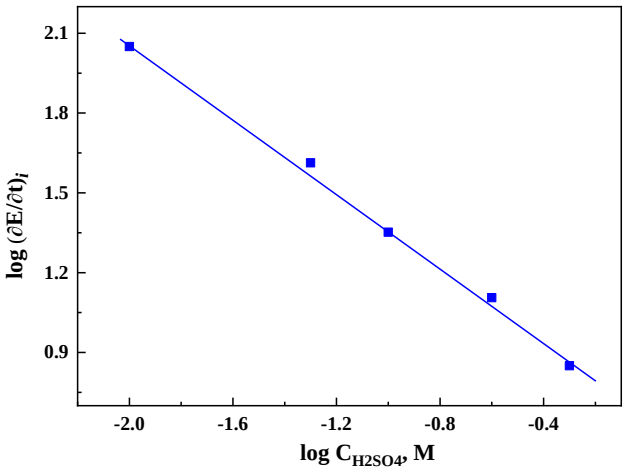

Figure 12. Variation of the rate of oxide film growth, $(\partial E/\partial t)_i$ with the concentration of H_2SO_4 on a double logarithmic scale.

3.3. The influence of temperature

The influence of temperature on the anodic dissolution and the passive film formation on Ni in $1x10^{-2}$ M H_2SO_4 solution, at a constant current density, was examined. Fig 13 depicts the effect of temperature (15-50°C) on the galvanostatic anodic polarization attitude of Ni in 0.01 M H_2SO_4 solution, at 1.0 $mAcm^{-2}$. The data indicate that the increase in the temperature extends the duration times required for the dissolution and the passivation processes while the rate of oxide film formation is reduced. The rise in the rate of nickel dissolution reaction and the decrease in the rate of oxide film formation by temperature could be attributed to the rise in the mobility of ions by temperature [59].

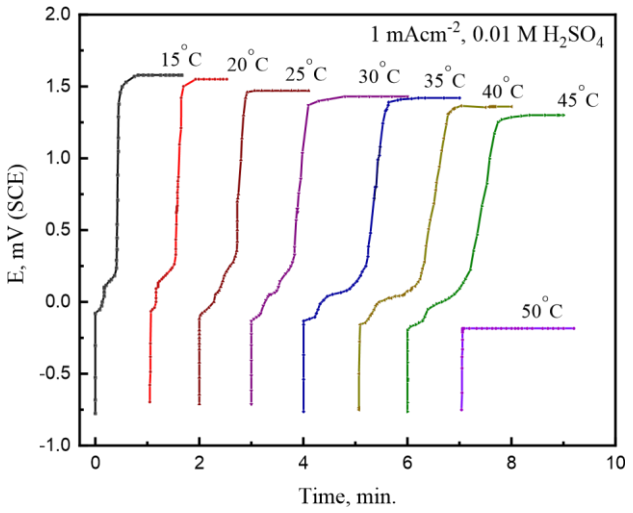

Figure 13. Effect of temperature on the anodic polarization curves of Ni in 0.01 M H_2SO_4 solution, at1 $mAcm^{-2}$.

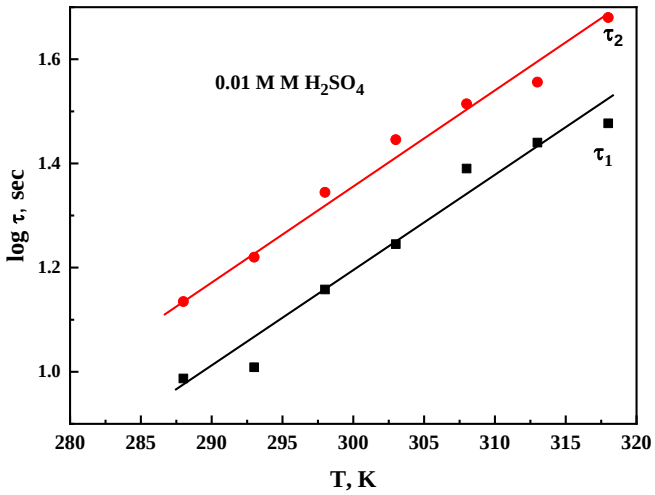

Figure. 14. Variation of logarithm of the duration time in sec (for the two arrests ***a*** and ***b***) with the absolute temperature, T, for Ni in 0.01 M H_2SO_4 solution, at 0.1mA/cm^2.

The intervals of each of the dissolution arrests ***a***, τ_1 and the passivation process, τ_2, are increased with rising temperature, while the oxide film formation is delayed. A linear relation between the logarithm of τ_1, and τ_2, with the solution temperature, T, confirms the direct proportional between the two variables as depicted in Fig 14. Also, the quantity of electricity, Q_a, consumed to reach passivity is increased with temperature. As the temperature is raised to 45°C the quantity of electricity, Q_a, consumed for passivation is increased to 80 mC/cm^2. Also, passivity does not attain at a temperature higher than 45°C, during the time of such an experiment. Such an attitude could be related to the rise in the rate of Ni dissolution, due to the diffusion of dissolved Ni^+ species away from the electrode surface. The rate of oxide film formation is decreased with temperature, owing to the possible solubility of the formed

surface oxide layer [55]. Early, Ammar and Khalil [57] reported the presence of two opposing processes competed on the metal surface; the anodic oxide repair and the oxide film dissolution. At low and intermediate temperatures, the rate of the oxide film formation is higher than the rate of metal dissolution, so the potential is shifted to higher values. The increase in temperature rises the rate of metal dissolution and prohibited oxide film formation. Recently, Park et al. related the rise in the dissolution rate of the passivated Ni with the solution temperature to the dissolution of the oxide film that thins locally and results in the ripping of the oxide layer [58].

However, the Arrhenius equation can be used to confirm the dependence of the rate of Ni metal dissolution and passivity formation on the temperature. Such an equation can be expressed as [26–28]:

$$\log r = \frac{-\Delta E_a}{2.303RT} + \log A \qquad (11)$$

where r represents the dissolution rate expressed in the interval of the dissolution step, τ, or the quantity of electricity consumed, Q_a consumed in oxide film formation. E_a is the apparent activation energy, T is the absolute temperature, A is a frequency factor and R is the universal gas constant.

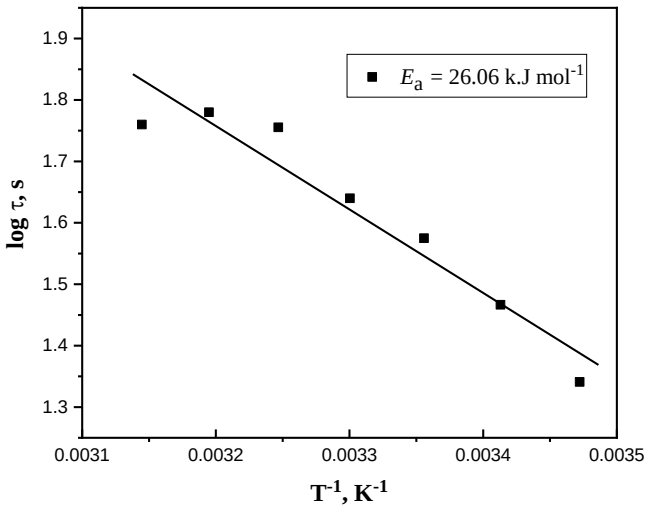

Figure. 15. Arrhenius plots for the variation of logarithm of the duration time required for oxidation process, τ, with the reciprocal of temperature, 1/T.

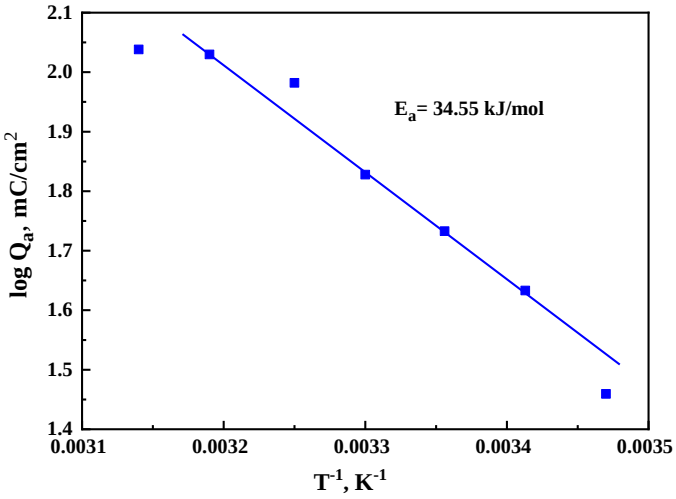

Figure. 16. Arrhenius plots for the variation of logarithm of the quantity of electricity required for passivation process, Q_a, with the reciprocal of temperature, 1/T.

The values of log *r* (s or mC/cm^2), obtained at different temperatures, confirm the linear relation of Figs 15 and 16 (plotting of log *r* against 1/T). The activation energy, E_a was deduced from the slope of the plots of Figs 15 and 16, and are tabulated in Table 5. The activation energy, E_a, for the dissolution was 26.06 kJ/mol while that of the passivation was 34.55 kJ/mol. The higher value for passivation confirms that the activation energy for the passivation process under the same experimental conditions are kinetically difficult than that of the dissolution processes.

Also, the transition state equation can be expressed by

$$r = \frac{RT}{Nh}\exp\left(\frac{\Delta S_a}{R}\right)\exp\left(\frac{-\Delta H_a}{RT}\right) \quad (12)$$

where *h* is Planck's constant and *N* is the Avogadro's number ΔH_a is the apparent enthalpy of activation, ΔS_a is the apparent entropy of activation, respectively. Plotting of log (*r*/T) against 1/T (Eq. 12) for The Ni dissolution and passivation in 0.01 M H_2SO_4 gave straight lines as depicted in Figs 17 and 18. The values of ΔH_a and ΔS_a are deduced from the slope of ($-\Delta H_a$/2.303R) and the intercept [log (R/Nh) + (ΔS_a/2.303R)] of the straight lines and are tabulated in Table 4. The positive sign of ΔH_a reflects the endothermic nature of the dissolution and passivation processes accompanied by the Ni metal dissolution and passivation in 0.01 M H_2SO_4 solution. The higher value of ΔH_a obtained with the passivation process would confirm that the passivation of Ni metal is a slow process. Besides, the negative sign in the values ΔS_a reflects the increase in disordering ongoing from reactants to the activated complex [49].

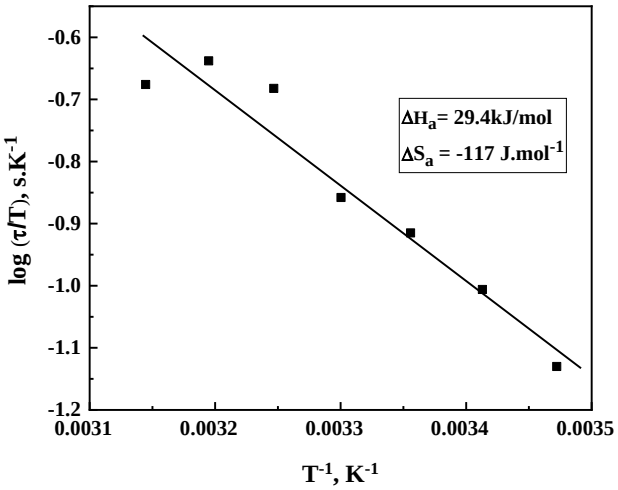

Figure 17. Transition state plots, for the duration of the dissolution process, log (τ/T), versus 1/T for Ni in 0.01 M H_2SO_4 solution at 0.1 mA/cm^2.

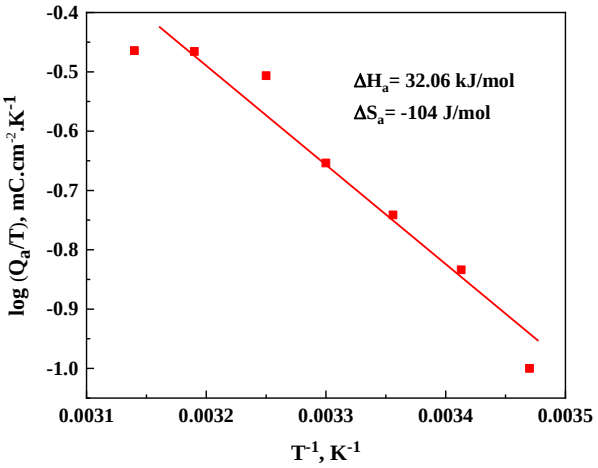

Figure 18. Transition state plots, for the quantity of electricity required for passivation process, log (Q_a/T) versus 1/T for Ni in 0.01 M H_2SO_4 solution, at 0.1 mA/cm^2.

Table 4. Thermodynamic activation corrosion and passivation parameters, E_a, ΔH_a and ΔS_a for Ni in 0.01 M H_2SO_4 solution, at 1.0 mA/cm^2.

Process	E_a, kJ mol^{-1}	ΔH_a, kJ mol^{-1}	ΔS_a, J mol^{-1} K^{-1}
dissolution	26.06	23.56	-136
Passivation	35.55	32.06	-104

4. CONCLUSION

The study of the galvanostatic anodic polarization of Ni in different concentrations of H_2SO_4 indicated that:

- Presence of two dissolution arrests confirming the oxidation of Ni into Ni^+ and Ni^{2+} ions followed by a linear rise in the potential due to passivity formation and oxygen evolution.

- The oxidation potential E_1 and E_2 are shifted to more positive values with rising the $I_{imposed}$, while the interval of the oxidation and passivation processes are lowered.

- The duration time, τ, of the two-oxidation steps are decreased with rising the $I_{imposed}$, T, and acid concentration, C.

- The thermodynamics activation parameters, E_a, and ΔH_a, confirmed that the transition state of the corrosion and passivation processes are endothermic processes.

- The oxide formation rate $(dE/dt)_i$ was directly proportional to the $I_{imposed}$ and inversely proportional to the acid concentration, *C*.

- The activation energies of the oxidation and passivation process were similar.

References

1. A.I. Mu˜noz, J.G. Anton, J.L. Gui˜non, V.P. Herranz, *Corros. Sci*., 48 (2006) 3349.
2. J. L. Trompette, L. Massot, H. Vergnes, *Corros. Sci.*, 74 (2013)187.
3. S.M. Abd El-Haleem, S. Abd El-Wanees, *Prot. Met. Phys. Chem*., 54 (2018) 859.
4. C. Xiaoliang, H. Ma, X. Chen, Corros. Sci., 42 (2000) 299.
5. M. Abdallah, A. Fawzy, H. Hawsawi, R.S.A. Hameed, S.S. Al-Juaid, *Int. J. Electrochem.* Sci., 15 (2020) 8129.
6. M. Abdallah, F. H. Al-abdali, R. El-Sayed, *Chem. Data Collect*., 28 (2020) 100407.
7. M. Abdallah, I. A. Zaafarany, S. Abd El Wanees and R. Assi, *Int. J. Electrochem. Sci*., 9 (2014) 1071.
8. G. Cordeiro, O. R. Mattos, O. E. Barcia, L. Beaunier, C. Deslouis, B. Tribollet, *J. Appl. Electrochem.*, 26 (1996) 1083.
9. M.R. Barbosa, J.A. Bastos, J. J. Garca-Jare˜no, F. Vicente, *Electrochim. Acta*, 44 (1998) 957.
10. S. M. Abd El-Haleem, S. Abd El-Wanees, *Mater. Chem. Phys*., 128 (2011) 418.
11. R. J. Smith, R. E. Hummel, J. R. Ambrose, *Corros. Sci*., 27 (1987) 815.
12. A. Seyeux, V. Maurice, L.H. Klein, P. Marcus, *Electrochim. Acta*, 54 (2008) 540.
13. F. Sun, G. Meng, T. Zhang, Y. Shao, F. Wang, C. Dong, X. Li, *Electrochim. Acta*, 54 (2009) 1578.
14. D. D. N. Singh and M. K. Banerjee, *Corrosion NACE*, 42 (1986)156.
15. W.T. Denholm, *Proc.1st Australain Conf. Electrochem., 1st Sydney, Hobart, Australia* 164 (1963).
16. R.P. Frankenthal, *J. Electrochem. Soc.*, 116 (1969) 1646.
17. R.P. Framkenthal, *J. Electrochem. Soc.*, 114 (1967) 542.
18. A.G. Akimov, Machavarianl, *1zv. Akad. Nauk, SSSR. Ser Khim*., 1 (1978)1482.
19. K. Schwabe, Z.G. Dietz, *Z. Electrochem*., 62 (1958) 751.

20. M. Hollnagal, Z. R. Landsberg, *Phys. Chem.*, 212 (1959) 127.
21. M. Pourbaix, *Atlas of Electrochemical Equilibria in Aqueous Solutions*, Pergamon Press, Oxford UK (1966) p.333.
22. S.C. Britton and U.R. Evans, *J. Chem. Soc.*, (1930) 1773.
23. E. Kunze and K. Schwabe, *Corros. Sci*., 4 (1964) 109.
24. J.O. Bockris, A. K. N. Reddy, and B. Rao, *J. Electrochem. Soc*., 133 (1966)1133.
25. G. Dibari, J.V.Petrocelli, *J. Electrochem. Soc*., 112 (1965) 99.
26. A. Pigeaud, *J. Electrochem. Soc.*, 122 (1975) 80.
27. S.S. Abd El Rehim, S. M. Abd El Wahab, and E.A.Abd El Megeed, *Surf. Coat. Technol.*, 29 (1985) 325.
28. A.H. Noorbakhsh Nezhad, A. Davoodi, E. Mohammadi Zahrani, R. Arefinia, *Surf. Coat. Technol*., 395(2020) 125946.
29. A.E. A. Skryleva, V. A. Bryukvin, T. B. Elemesov, A. M. Levin, *Russian Metallurgy* (*Metally*) 11 (2014) 865.
30. N. Sato and G. Okamoto, *J. Electrochem. Soc.* 110 (1963) 605.
31. S. Abd El Wanees, M.I. Alahmdi, M.A. Alsharif, Y. Atef, *Egyp .J. Chem*., 62 (2019) 811.
32. M.G.A. Saleh, S.Abd El Wanees, S. Khalid Mustafa, *Chem. Eng. Commun*., 206 (2019)789.
33. S. Abd El Wanees, S.H. Seda, *J. Disper. Sci. Technol*., 40 (2019) 1813.
34. S. Abd El Wanees, E. E. Abd El Aal, *Corros. Sci*., 52 (2010) 338.
35. F. M. Abd El wahab, J. M.Abd El kader, H. A. El shayed, A. M. Shams El Din, *Corros. Sci*., 18 (1978) 997.
36. E. E. Abd El Aal, *Corroion NACE*, 55 (1999) 582.
37. E. E. Abd El Aal, *Corros. Sci.*, 48 (2006) 343.
38. E.E.Abd El Aal and S. Abd El Wanees, *Corros. Sci.*, 51 (2009) 458.
39. E.E.Abd El Aal, *J. Power Sources* 102 (2001) 233.
40. B. Mac Dougal, D.F. Mitchell, M. J. Graham, *J. Electrochem. Soc*., 127 (1980) 1248.
41. M. Pourbaix, *Atlas of Electrochemical Equilibria, Pergamon Press, Oxford, UK* (1996) p.330.
42. R. Nishimura, M. Araki, and K. Kudo, *Corrosion NACE*, 43 (1987) 486.
43. E.E. Abd El Aal, *J. Power Sources*, 75 (1998) 36.
44. Z. Grubač, Ž. Petrović, J. Katić, M. Metikoš-Huković, and R. Babić, *J. Electroanal. Chem.*, 645 (2010) 87.
45. C. A. Melendres, and M. Pankuch, *J. of Electroanal. Chem*., 333(1992) 103.
46. L.J. Oblonsky, T. M. Devine, *J. Electrochem. Soc.*, 142 (1995)3677.
47. G. Okamoto, N. Sato, *Trans. Jap. Inst. Met*., 1 (1960) 16.
48. N. Sato and G. Okamoto, *J. electrochem*. Soc., 110, (1963) 605.
49. N. Sato and G. Okamoto, *Trans. Jap. Inst. Met*., 2 (1961) 113.
50. E. E. Abd El Aal, *Corros. Sci*. 42(2000)1.
51. I. A. Ammar, S. Darwish, W.W. Khalil, and S. El Taher, *Corrosion NACE*, 46 (1990) 197.
52. I. A. Ammar, and A. Saad, *J. Electroanal. Chem. & Interfacial Electrochem.*, 34 (1972) 159.
53. S.M. Moon, and S.-I. Pyun: 44 (1999) 244.
54. S. Darwish, *Corrosion NACE*, 27 (1971) 265.
55. E.E. Abd El Aal, *Corros. Sci.*, 45 (2003) 641.
56. E.E. Abd El Aal, *Corros. Sci*., 45 (2003) 759.
57. I. A. Ammar, and M. W. Khalil, *Electrochim. Acta*, 16 **(**1971)1601.
58. F. Lallemand, F.P lumier, J. Delhalle, and Z.Mekhalif, *Appl. Surf. Sci.*, 254 (2008) 3318.
59. S.S. Zumdahl, *Chemistry, 3rd* Ed, D.C. Heath & Co. (1993) p. 645.